Creep-Fatigue Interactions in P91 Steel

Magdalena Speicher[1,*], Andreas Klenk[1], Kent Coleman[2]

[1] Materialpruefungsanstalt Universitaet Stuttgart, Stuttgart 70569, Germany
[2] Electric Power Research Institute, Charlotte NC 28262, USA
* Corresponding author: magdalena.speicher@mpa.uni-stuttgart.de

Abstract To determine and quantify the influence of creep-fatigue interactions on the crack behaviour of P91 steel creep-fatigue crack growth (CFCG) tests were carried out with holding times up to 60 minutes and compared to results from fatigue crack growth (FCG) and creep crack growth (CCG) tests.
It was found that the introduction of a holding time influences the crack initiation time but not the crack propagation. With holding times of 60 minutes, the difference between CCG and CFCG tests is very small.
To characterise the fracture mode metallographic analyses were performed on selected specimens after CFCG tests. The crack path is inter-granular and an area of high cavity density was identified around the crack tip in all specimens. By comparing CFCG, FCG and CCG results, it can be finally noticed that specimens with a holding time of 6 and 60 min show a similar crack growth rate as samples under creep loading.

Keywords martensitic steel, creep-fatigue, crack initiation, crack growth

1. Introduction

In components operated at high temperature, there is always some amount of interaction between fatigue, creep and the environment. This is typically the case in power plants where steam generating service start-ups or load changes produce changes in steam conditions and transient temperatures. In the last decades, it has been proven that in the creep-fatigue range, the lifetime of components is significantly shorter, particularly when hold periods are introduced between strain cycles. These interactions can be enhanced due to environmental effects such as for instance internal or surface oxidation. They are finally more pronounced for some materials, can be neglected for others. In this work, the crack behaviour of the steel P91 was investigated in creep-fatigue tests. The aim of this analysis is to gain information about how the crack behaviour of this steel is influenced by creep-fatigue-environment interactions at high temperature.

2. Experimental Details

2.1. Material

The base material P91 (X10CrMoVNb9-1) being under investigation, comes from a thick pipe with outer diameter of 492 mm and wall thickness of 85 mm. Its chemical composition is given in Table 1. These values are in accordance with the EN10216 requirements [1]. The P91 pipe was used in [2] for the investigation of similar welds under creep conditions. A classical Post Weld Heat Treatment (PWHT) was therefore used to relax the stresses that were induced by the welding process.

Table 1. Chemical composition of P91 used in this work

		Chemical composition in mass (%)										
		C	**Si**	**Mn**	**P**	**S**	**Cr**	**Mo**	**Ni**	**Al**	**Nb**	**V**
[1]	Min	0,08	0,20	0,30	-	-	8,0	0,85	-	-	0,06	0,18
	Max	0,12	0,50	0,60	0,02	0,010	9,5	1,05	0,40	0,04	0,10	0,25
this work	Meas.	0,104	0,27	0,46	0,014	0,003	8,17	0,9	0,16	0,02	0,064	0,194

In order to optimize the full-use of the already acquired database, the P91 samples investigated in this work where submitted to the same heat treatment as follows: austenitising at 1050°C for 10 min with air cooling, tempering at 750°C for 70 min and PWHT at 760°C for 2 h as it is often performed for components with welds.
The microstructure of P91 consists of tempered martensitic, see Fig. 1. During creep, fatigue or creep-fatigue interactions, the microstructure of such steels is instable. A drop in the dislocation density, an augmentation of the subgrain size leading to an equiaxial microstructure and a growth in the size of precipitates such as carbides $M_{23}C_6$ ($Cr_{23}C_6$) and carbonitrides MX (VN, VC, NbC) in the matrix are influencing the global deformation behaviour.

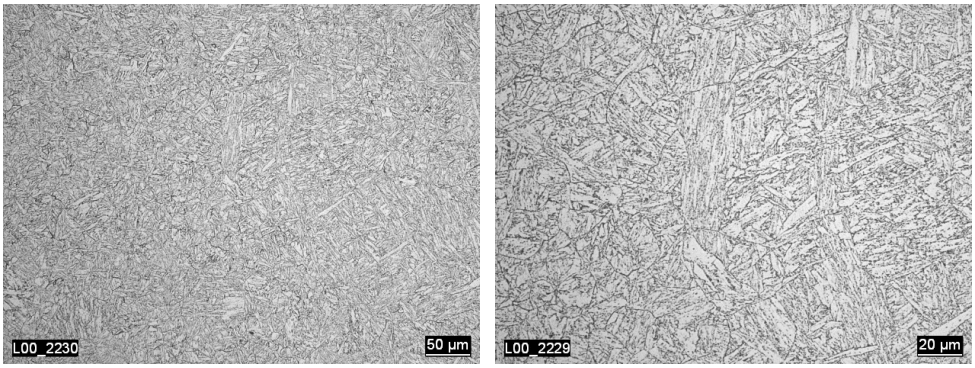

Figure 1. Microstructure of P91-steel, light optical images

2.2. Mechanical testing

For the crack growth tests side-grooved Compact Tension specimens C(T)-25 were used. The starter notch was realised by fatigue pre-cracking. All samples have an a_0/W-ratio in the range of 0.52 to 0.60. Creep Crack Growth tests (CCG) were performed according to ASTM E 1457-07 [3]. Creep-Fatigue Crack Growth tests (CFCG) were performed with a load ratio $R = F_{min}/F_{max}$ of 0.1 and with hold periods at maximum load of 6 and 60 min according to ASTM E 2760-10 [4]. Fatigue Crack Growth tests (FCG) were performed with a load ratio R = 0.1 and frequency of 0.5 Hz. All tests were carried out at 580°C and 600°C.
During the tests, the load line displacement was measured by means of capacitive high temperature strain gauges. The crack propagation was monitored online using the Alternating Current Potential Drop (ACPD) technique. At the end of each experiment, the potential drop signal was calibrated with the final crack length measured on the fractured specimens. For this, the specimen was broken up under liquid nitrogen after the test and the crack length was measured according to [3].

3. Description of crack initiation and crack propagation under creep and fatigue conditions

Crack initiation and crack propagation under creep conditions can be described by the usual fracture mechanics parameter C* and the stress intensity factor K_I.
- In linear-elastic fracture mechanics the stress intensity factor K_I is generally used for components with predominantly linear-elastic behaviour. Only a small plastic or creep zone at the crack tip can be assessed using this parameter. For side grooved C(T)-specimens the stress intensity factor is calculated as:

$$K_I = \frac{F}{\sqrt{B \cdot B_N \cdot W}} \cdot \left(2 + \frac{a}{W}\right) \cdot f\left(\frac{a}{W}\right) \quad (1)$$

$$f\left(\frac{a}{W}\right)=\frac{\left[0.886+4.64\cdot\left(\frac{a}{W}\right)-13.32\cdot\left(\frac{a}{W}\right)^2+14.72\cdot\left(\frac{a}{W}\right)^3-5.6\cdot\left(\frac{a}{W}\right)^4\right]}{\left(1-\frac{a}{W}\right)^{1.5}} \tag{2}$$

where F is load, B is specimen thickness, B_N is net thickness of side grooved specimens, a is crack length and W is test piece width.

- Components with stationary creep (not only at the crack tip) are assessed using the integral C*. In case of the experimental determination of the parameter C* approximation formulae can be used for a number of fracture mechanics specimens [5], which are basically functions of the load line displacement rate due to creep [3]:

$$C^* = \dot{v}_C \cdot \sigma_{net} \cdot \eta \tag{3}$$

with load line displacement rate $\dot{v}_C$, net section stress σ_{net} and the factor η depending on specimen geometry (η = [2+0.522•(1-a/W)] for C(T)-specimens).

For the evaluation of C(T)25-specimens the following equation was used:

$$C^* = \dot{v} \cdot \frac{F}{B_N \cdot c} \cdot \frac{h_1}{h_3} \cdot \frac{W/a-1}{\beta \cdot \eta} \tag{4}$$

where h_1 and h_3 are geometrical functions, c=W-a, and β: 1,071 for plain stress condition.

One of the validity criteria, which decide on the suitability of the relevant parameter, is the transition time t_1 [3]:

$$t_1 = \frac{K_I^2}{C^* \cdot (n+1) \cdot E'} \tag{5}$$

If t_1 is smaller than the crack initiation time $t_1 << t_i$ for the initiation criterion (Δa_i=0.5 mm) the parameter C* is more appropriate for the description of crack behaviour under creep conditions.

In order to describe the creep crack growth rate either the parameters C* or stress intensity factor K_I can be used, dependent on the situation in the component. Typically, the creep crack growth rate depending on the respective fracture mechanics parameter is presented as follows:

$$\frac{da}{dt} = C_1 \cdot (K_I)^{m_1} \tag{6}$$

$$\frac{da}{dt} = C_2 \cdot (C^*)^{m_2} \tag{7}$$

where C_1, C_2, m_1 and m_2 are material constants.

Fatigue crack behaviour can be described by threshold values for the beginning of cyclic crack growth and by the Paris-law [6] for the crack propagation:

$$\frac{da}{dN} = C_3 \cdot (\Delta K)^{m_3} \tag{8}$$

with C_3 and m_3 as material specific constants.

3. Results and Discussion

3.1. Crack initiation under creep-fatigue loading

The results of creep-fatigue crack growth tests as a function of stress intensity factor and initiation time are shown in Fig. 2 a compared to the creep crack growth tests and in Fig. 2 b compared to fatigue crack growth tests. In addition, the literature data from [7] are shown there.
An effect of holding time (HT) on the creep crack initiation time for the technical initiation criterion (Δa_i=0.5 mm) is observed, whereby the influence of HT of 6 min for both test temperatures is greatest. For lower loaded sample at 600°C (HT=6 min), the influence of the holding period on the initiation time is significantly lower than for the higher loaded specimen. This indicates the time-dependence during the holding period and the creep process seems to be dominant. If the holding time is one hour, the difference between the results of creep crack growth test and creep-fatigue crack growth test is small, especially at 600°C. The differences between the two specimens with short and long holding time at 580°C are not significant. This means that a reduction in time is expected due to cyclic stress for crack initiation. Literature data from [7] show no influence of the holding time on crack initiation time, so that these results can be described independently of the holding time by the creep curve in the investigated area (see Fig. 2 a).
Fig. 2 b shows the dependency of the cyclic stress intensity factor as a function of the number of cycles to crack initiation at Δa_i = 0.5 mm. It can be seen that the creep-fatigue specimens with short holding times are closer to the experiments under pure cyclic loading.

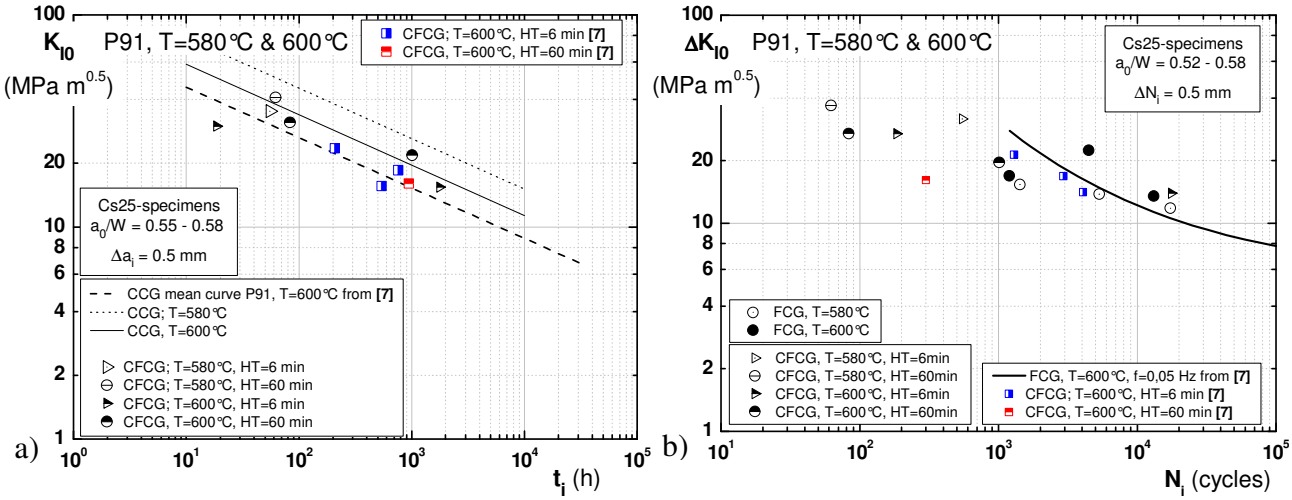

Figure 2. a) Stress intensity factor K_{I0} over time for Cs25-specimens (T=580°C & 600°C) under creep-fatigue loading compared to P91-steel mean curve for creep at 600°C from [7]; b) Cyclic stress intensity factor ΔK_{I0} over cycles for Cs25-specimens (T=580°C & 600°C) under creep-fatigue loading compared to the results under fatigue loading at 580°C and 600°C

In Fig. 3 the parameter C* is shown depending on the time to the crack initiation (determined at Δa=0.5 mm) under creep-fatigue condition. As expected, the creep-fatigue samples with longer holding periods are closer to the curve of creep crack growth tests.

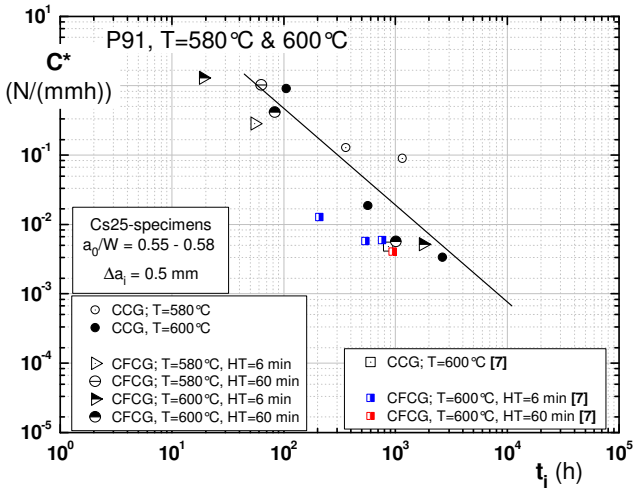

Figure 3. C* parameter over time for Cs25-specimens (T=580°C & 600°C) under creep-fatigue loading compared to P91-steel from [7]

3.2. Crack propagation under creep-fatigue loading

The comparison of CFCG- and CCG-experimental results shows (see Fig. 4 a and Fig. 4 b) that the specimens with a holding time of 6 min and 60 min have similar crack growth rates as samples without holding time, regardless of which of the two parameters describing the crack behaviour is used. No influence of holding time on crack initiation as described in the last section is observed for crack propagation. Thus, the cyclic loading has only an influence on the crack behaviour in the initial phase. In the holding time period the creep loading is dominant. Metallographic studies confirmed this observation so far (see next section).

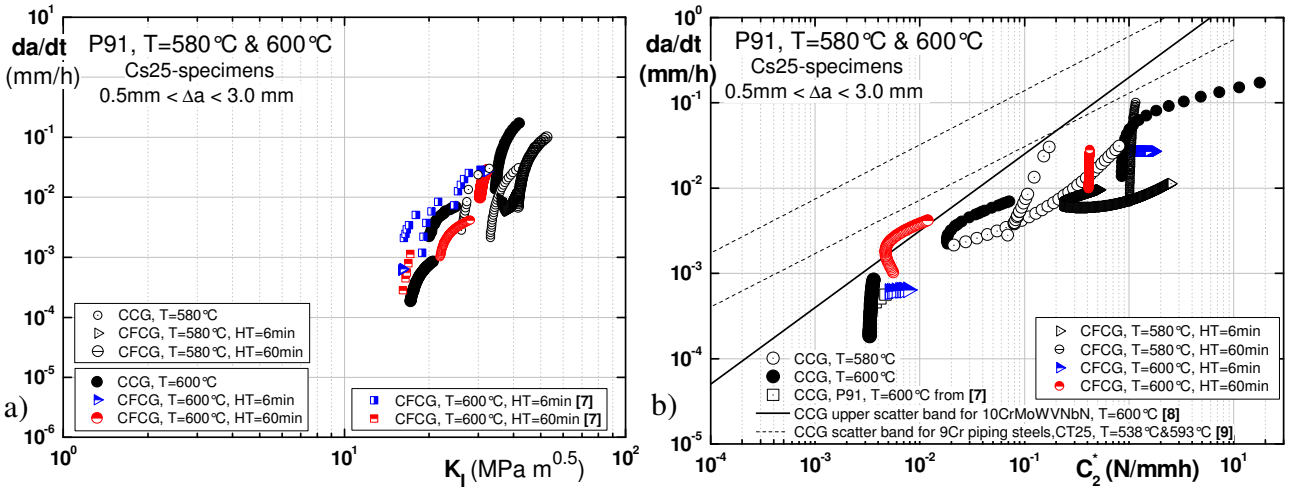

Figure 4. Creep-fatigue crack growth rate over a) stress intensity factor K_I and b) parameter C* for Cs25-specimens (T=580°C & 600°C) compared to literature data from [7-9]

In Fig.5 the results of fatigue crack growth tests at 580°C and 600°C are reported. The influence of temperature on the fatigue crack growth behaviour can be seen. The fastest crack growth rates are observed at 600°C. The results obtained in this work are similar to literature data from [9] for P91 at 565°C and a frequency f of 0.1 Hz. One sample at 600°C is slightly above the Paris-law curve, which can be explained by the different test temperature. It is also evident that results of CFCG-tests at 580°C and 600°C cannot be described by the Paris-law. The cyclic crack-growth rate increases if a hold time is imposed at maximum load. As the hold time increases, a change from cycle dependent to time dependent behaviour can be observed.

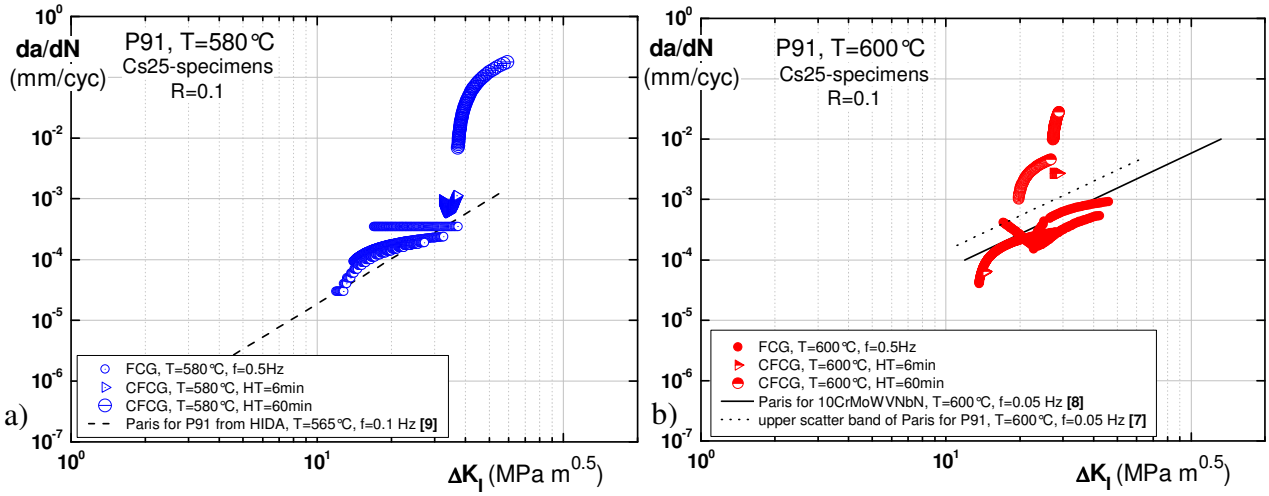

Figure 5. Creep-fatigue crack growth rate over ΔK_I for Cs25-specimens at a) T=580°C and b) T=600°C compared to literature data from [7-9]

3.4. Metallografic investigations

In Fig. 6 and Fig. 7, the crack paths for selected specimens of different crack growth tests are shown. A comparison of CCG-tests and CFCG-tests with a short and long holding time of 6 min and 60 min and under fatigue loading shows the different mechanisms that play a significant role in the crack propagation process.

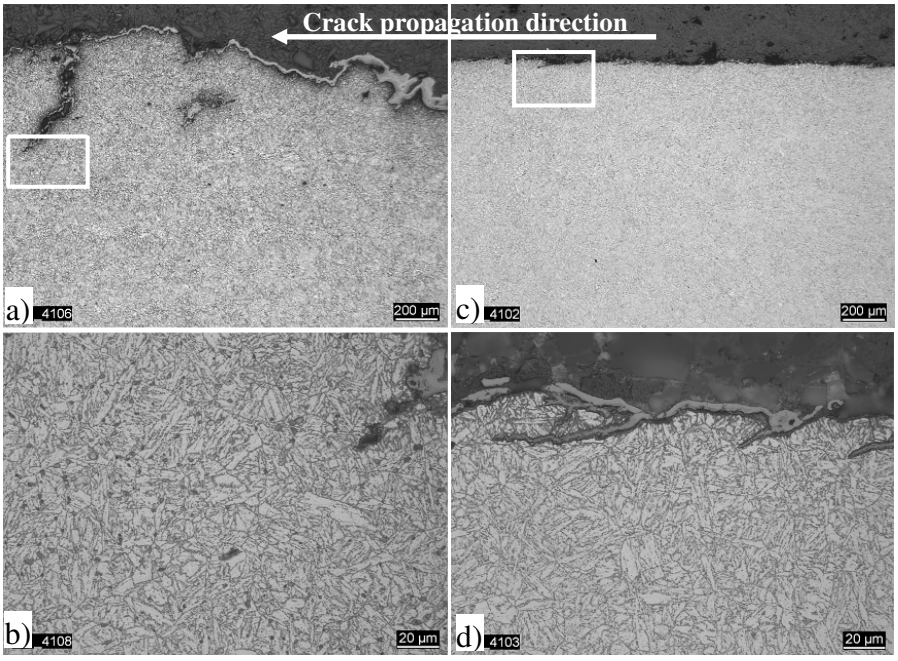

Figure 6: a) Specimen after CCG-test at 600°C, b) detail view from a); c) Specimen after FCG-test at 600°C, d) detail view from c)

A large amount of creep cavities is found on the prior austenite grain boundaries at the crack tip and along the crack path of a creep crack growth tested specimen (see Fig. 6a and b). Due to the strong oxidation of the crack surface, the crack cannot be clearly identified as inter-granular. Nevertheless, by comparing this specimen with the sample tested under pure fatigue loading (see Fig. 6 c and d), it is clear that the crack paths are different. This was already visible on the fracture surface. The surface of the specimen tested under fatigue loading was smooth, which suggests that the crack was

propagating trans-granular. This has been confirmed in an light-optical investigation of a cross section.

For the samples tested under creep-fatigue loading (see Fig. 7) the crack behaviour was found to be independent on the holding time similarly like specimens tested under creep loading (Fig. 6 a, b). Around the crack tip an area of high cavity density was identified and the crack path under creep-fatigue loading is comparable with the crack path under pure creep condition. Also along the crack path creep cavities were observed.

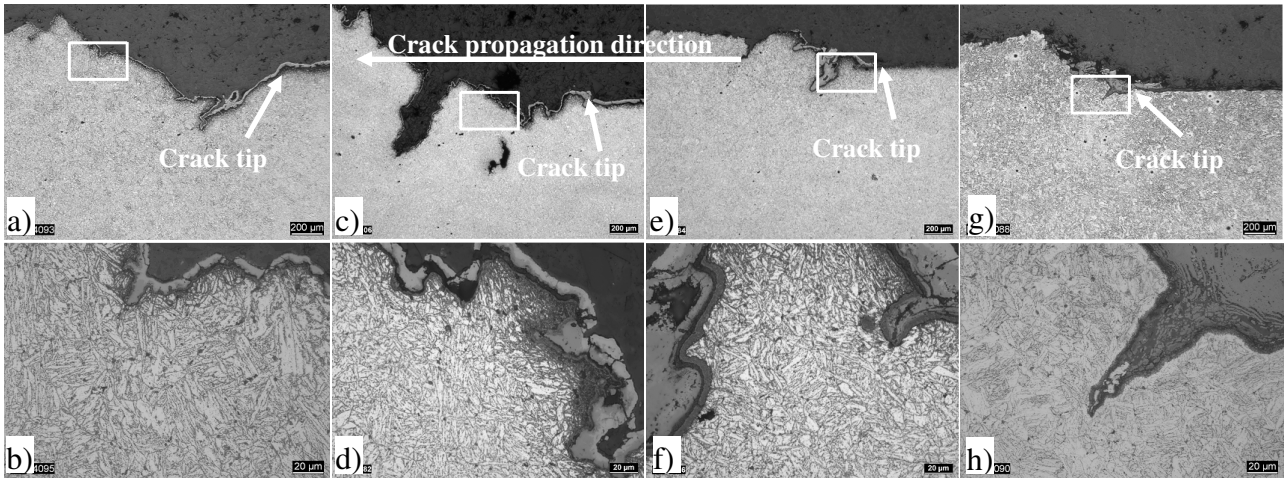

Figure 7: Specimen after CFCG-test at 580°C with a), b) HT=6 min (b) detail view from a)), c), d) HT=60 min (d) detail view from c)), at 600°C with e), f) HT=6 min (f) detail view from e)), g), h) HT=60 min (h) detail view from g))

3.3. Creep-fatigue interactions

The crack propagation rate da / dN under creep-fatigue loading is influenced by two failure mechanisms, and therefore depends on the load level, the mean stress, the stress ratio R and the temperature. Generally, there are three different areas [10]. At high frequencies, the crack growth per cycle is independent of frequency, because the cycle duration is so short that no time remains for creep crack growth. With decreasing frequency, the crack growth per cycle da / dN is greater. The time between two load cycles is then sufficiently large, so that fatigue crack growth and creep crack growth can overlap. With further decreasing frequency of the fatigue crack propagation loses its meaning. The crack propagation is now determined only by creep crack growth.

In literature [11, 12] different relationships exist to describe the crack growth under creep-fatigue loading, for example the following equation recommended for creep-ductile materials (see also [4]):

$$\frac{da}{dN} = C_0(\Delta K)^{n0} + \int_0^{t_h} C_1((C_t)_{avg})^q dt \tag{9}$$

According to [11] the final equation can be:

$$\frac{da}{dN} = C_0(\Delta K)^{n0} + C_1 K^{2m} t_h^{\,1-m} + C_2 C^{*m} t_h \tag{10}$$

with t_h as holding time. The first term is a pure-fatigue contribution reflecting no effect of hold time and corresponding to crack-growth behaviour at short hold times and high frequencies. This term can be evaluated if the Paris-law coefficients are available. For further evaluation, the coefficients from Table 2 will be used. The second term shows a nonlinear power-law dependence of

crack-growth rate on hold time and pertains to intermediate hold times and frequencies where creep-fatigue interaction is present. The coefficient C_1 was adopted from literature data for 1CrMoV-steel and 304 stainless steel [11]. A value between 10^{-7} and 10^{-6} for different materials at high temperature was found to be appropriate. For further evaluations a value of 10^{-6} was assumed, see Table 2. The third term including the C* parameter shows a linear dependence of crack growth on hold time and corresponds to purely creep-dominated crack growth occurring at long hold times and low frequencies [11]. Using the solutions for stress intensity factor K, and C* by appropriate Norton-law coefficients, the values from Table 2 are applied for the assessment.
With the accumulation rule according to Eq. (10) the results of creep-fatigue tests on P91-steel were evaluated under creep-fatigue loading and $R = F_{min} / F_{max}$=0.1. The assessment was carried out for C(T)-25 samples with a_0/W – ratio of 0.55.

Table 2. Material related parameters for describing the crack growth rates of P91

		Fatigue		Interaction		Creep	
		C_0	n_0	C_1	m	C_2	m
Eq. 10	580°C	8,85E-08	2,49	1E-06	0,66	4,21E-02	0,66
	600°C	8,85E-07	1,91				
Eq. 11	580°C	8,85E-08	2,49	-	-	6,17E-13	0,70
	600°C	8,85E-07	1,91	-	-		

The comparison between calculated and experimentally determined values is shown in Fig.8. The calculated values are overestimated for both temperatures and holding times. The creep portion is dominant in this case, so that the crack growth can be described based on creep only using C*. The biggest uncertainty here is the determination of C* with the Norton-approach, as the results are strongly influenced by changes in the Norton coefficients.

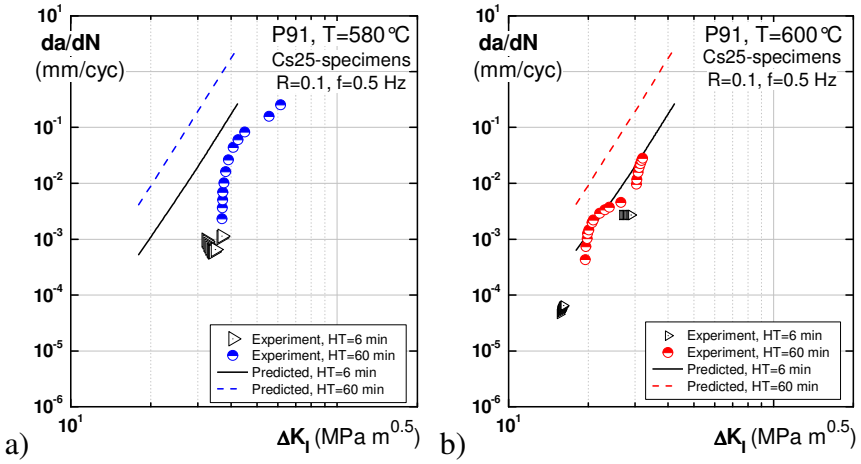

Figure 8. Creep-fatigue crack growth rate over ΔK_I for Cs25-specimens at a) T=580°C, b) T=600°C

Another commonly used approach based also on simple linear superposition of creep crack growth and fatigue crack growth is the model applying the fracture mechanics parameters ΔK for fatigue load and K for creep load [7]:

$$\frac{da}{dN_{CFCG}} = \frac{da}{dN_{FCG}} + \frac{1}{f} \cdot \frac{da}{dt_{CCG}} = C_0 (\Delta K)^{n0} + C_2 K^m \cdot t_h \qquad (11)$$

The results of the evaluation by this rule are shown in Fig. 9. It can be seen that this approach describes the behaviour under creep-fatigue loading much better, although the material is creep-ductile. At 580°C and the hold time of 6 min the influence of the fatigue proportion on the

crack growth can be recognize. For a holdtime of 60 min it is obviously that the behaviour is time dependent. At 600°C and both holding times, it is apparent that the rule describes the crack growth behaviour of creep-fatigue specimens quite well. Fig. 9e shows the dependence on the crack growth rate at 600°C on the holding time for a constant value of ΔK=27.2 MPam$^{0.5}$. In this case, the cycle/time dependent transition for this material can be expected at holding times greater than 0.1 minutes.

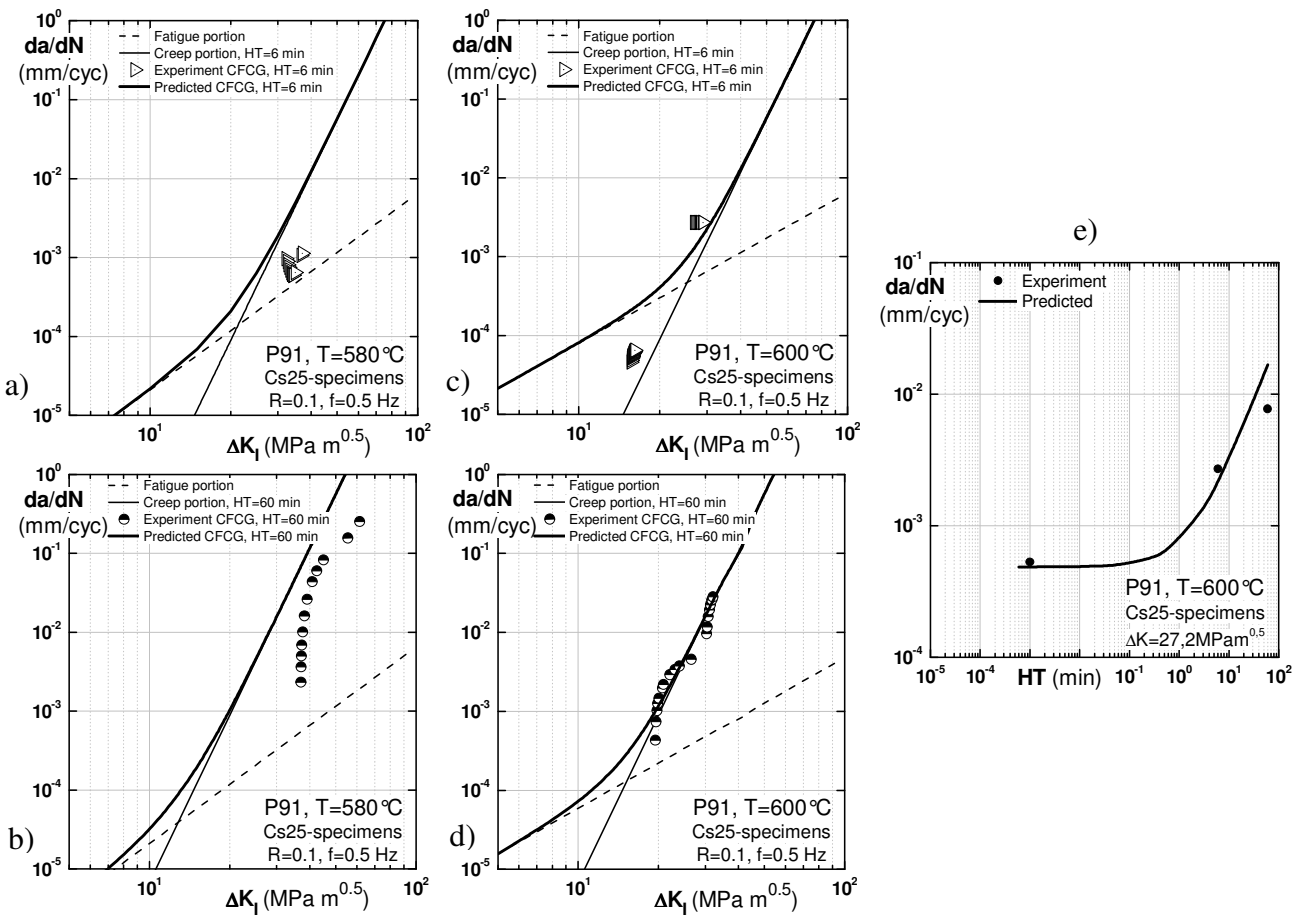

Figure 9. Creep-fatigue crack growth rate over ΔK_I for Cs25-specimens at a)&b)T=580°C, c)&d) T=600°C, e) Creep-fatigue crack growth rate over holding time for ΔK_I =27.2 MPam$^{0.5}$ at 600°C

4. Summary

The results of investigations on P91-steel show, that the creep crack initiation behaviour can be described by the parameter C* and by the stress intensity factor K_I. Due to the high creep ductility of P91 the C*-parameter is preferable. An effect of holding time (HT) on the creep crack initiation time is observed, whereby the influence of 6 min HT for both test temperatures is greatest. If the holding time is 60 min the difference between the creep crack growth test and creep-fatigue crack growth test is small, especially at 600°C. At 580°C the influence of short and long holding time on the crack initiation time for two creep-fatigue experiments is comparable. This means that a reduction in time is expected due to the cyclic stress for the crack initiation in the investigated range.

The crack propagation behaviour of P91-steel under creep conditions can be described both by the parameter C* and the stress intensity factor K_I. The Paris-law describes fatigue crack propagation. An influence of the temperature on crack propagation under fatigue loading can be observed, crack growth rate increases with increasing temperature. By comparing CFCG- and CCG-experimental

results, it can be noticed that specimens with a hold time of 6 min and 60 min have similar crack growth rate as samples without holding time, regardless of which of the two parameters describing the crack behaviour is used. Contrary to the influence of hold time on crack initiation almost no influence is observed on crack propagation. Hence, cyclic loading has only an influence on the crack behaviour in the initial phase. In the holding period creep loading is dominant.
Metallographic analyses show that the crack propagates inter-granularly under creep load and a large amount of cavities are found on the prior austenite grain boundaries near to the crack tip. Under fatigue loading trans-granular cracks without cavities were observed. For the samples tested under creep-fatigue loading the crack behaviour was found to be independent of the holding time. Around the crack tip an area of high cavity density was identified and the crack path under creep-fatigue loading is comparable to the crack path under creep condition.
The crack propagation under creep-fatigue loading is influenced by two failure mechanisms, and therefore depends on the load level, the mean stress and the temperature. With decreasing frequency the mechanisms changes from cycle dependent at high frequencies to time dependent at lower frequencies. In literature, different relationships exist to describe the crack growth under creep-fatigue loading, which were investigated in this study. It has been shown that the accumulation rule based on stress intensity parameter K_I better describes the crack growth behaviour of P91 under creep-fatigue loading. If the creep portion is described by parameter C*, the crack growth behaviour is overestimated. This may be the effect of the relatively large scatter of experiments data, or may result from uncertainties in the determination of C*.

Acknowledgements

The authors gratefully acknowledge the financial support provided by EPRI, Charlotte, USA.

References

[1] DIN EN10216: 09 Seamless steel tubes for pressure purposes - Technical delivery conditions - Part 1: Non-alloy steel tubes with specified room temperature properties; German version prEN 10216-1:2009.
[2] H. Theofel, K. Maile, Untersuchung einer artgleichen Schweißverbindung für 9%Cr1%Mo-Stähle unter besonderer Berücksichtigung des Langzeitkriechverhaltens, AiF Report Nr. 9300, 1997.
[3] ASTM E 1457-07, Standard Test Method for Measurement of Creep Crack Growth Rates in Metals, 2007.
[4] ASTM E 2760-10, Standard Test Method for Creep-Fatigue Crack Growth Testing, 2010.
[4] H. Riedel, Fracture at High Temperatures, Springer-Verlag, 1987.
[6] P.C. Paris, M.P. Gomez, W.E. Anderson, A Rational Analytic Theory of Fatigue, The Trend in Engineering, 13 (1961) 9-14.
[7] C. Berger, E. Roos, et al., Rissverhalten typischer warmfester Kraftwerksbaustähle im Kriechermüdungsbereich, Final report of AiF-Project Nr. 10395, 1999.
[8] E. Roos, C. Berger et al., Kriech- und Kriechermüdungsrissverhalten moderner Kraftwerkstähle im Langzeitbereich, Final report of AVIF-Project Nr. A178, 2006.
[9] Validation, Expansion and Standardisation of Procedures for High Temperature Defect Assessment (HIDA), Brite/Euram Project: BE1704, Final Report 1999.
[10] M. Pfaffelhuber, M. Rödig, F. Schubert, H. Nickel, Risswachstum unter überlagerter Kriech- und Ermüdungsbelastung in X10NiAlTi 32 20 (Alloy 800), Report of Kernforschungsanlage Jülich Nr. 2303, 1989.
[11] R. Viswanathan, Damage Mechanisms and Life Assessment of High-Temperature Components, AMS International, 1989.
[12] J.M. Larson, Th. Nicholas, Cumulative-Damage Modelling of Fatigue Crack Growth in Turbine Engine Materials, Engineering Fracture Mechanics, 22 (1985) 713-730.